Theoretical Model of Two-Phase Flow in a Nozzle and Its Application to Numerical Experiments for Mist Flow

AUTHOR(S):

HATTA, Natsuo; KOKADO, Jun-ichi; ISHII, Ryuji; FUJIMOTO, Hitoshi

CITATION:

HATTA, Natsuo ...[et al]. Theoretical Model of Two-Phase Flow in a Nozzle and Its Application to Numerical Experiments for Mist Flow. Memoirs of the Faculty of Engineering, Kyoto University 1989, 51(2): 73-107

ISSUE DATE:

1989-04-30

URL:

http://hdl.handle.net/2433/281392

Theoretical Model of Two-Phase Flow in a Nozzle and Its Application to Numerical Experiments for Mist Flow

By

Natsuo HATTA*, Jun-ichi KOKADO**, Ryuji ISHII*** and Hitoshi FUJIMOTO****

(Received November 25, 1988)

Abstract

A numerical analysis of subsonic as well as supersonic nozzle flows of gas-particle mixtures is described. The theoretical model modified here is applied to the case where a gas-particle mixture is composed of air and water-particles in relation to the mist nozzle flow utilized for the secondary cooling zone of a continuously cast slab. For the subsonic nozzle flow, all of the flow properties are calculated on the basis of a given nozzle geometry with a parallel region. Next, for the supersonic nozzle, the so-called specified pressure method is applied to evaluate the behaviour of the gas-particle mixture in the flow field, as wel as to design the converging-diverging nozzle configuration according to the desired pressure profile. The results so obtained are examined and discussed from a numerical point of view.

Nomenclature

a	= dimensionless local sonic speed
A	= dimensionless sectional area of nozzle
A_{p0}	= dimensionless friction factor defined in Eq. (55)
C_D	= drag coefficient
$\overline{c}_{pg}$	= gas specific heat at constant pressure
$\overline{c}_{pp}$	= specific heat of particle material
f_p	= momentum transfer parameter defined in Eq. (16)
g_p	= heat transfer parameter defined in Eq. (21)
$\overline{h}$, $\overline{h}_p$	= enthalpy for gas and particle, respectively

* Dept. of Mineral Science and Technology, Faculty of Eng., Kyoto Univ., Kyoto 606
** Niihama College of Technology, Niihama 792
*** Dept. of Aeronautical Eng., Faculty of Eng., Kyoto Univ., Kyoto 606
**** Graduate Student, Kyoto Univ., Kyoto 606

$\overline{H}$, $\overline{H}_p$ = stagnation enthalpy for gas and particle, respectively
K_p = constant velocity lag factor defined in Eq. (78)
L = dimensionless nozzle radius
$\bar{l}_p$ = average particle radius ($\bar{l}_p \equiv \bar{l}_p(\bar{x})$)
L_p = constant thermal lag factor defined in Eq. (79)
$\overline{L}_*$ = nozzle radius at throat
$\dot{m}_p$ = dimensionless mass flow rate function of particle defined in Eq. (50) ($\dot{m}_p \equiv \dot{m}_p(r_p)$)
M = local gas-phase Mach number
$\dot{M}_g$, $\dot{M}_p$ = dimensionless total mass flow rate of gas and particle, respectively, defined in Eqs. (46) and (47)
n_p = dimensionless number density function of particle ($n_p \equiv n_p(r_p)$)
N_p = $\int n_p(r_p)dr_p = \overline{N}_p / \overline{N}_{p0}$ (see Eq. (10))
Nu = particle Nusselt number defined in Eq. (19)
p = dimensionless pressure
$\overline{p}_e$ = ambient gas pressure at nozzle exit
Pr = gas-phase Prandtl number
Re_p = particle Reynolds number defined in Eq. (56)
r_p = dimensionless particle radius ($= \overline{r}_p / \bar{l}_{p0}$)
$\overline{R}_p$ = density of condensed particle per unit volume of flowing medium
$\overline{r}_{p,max}$ = maximum radius of particle
$\overline{r}_{p,min}$ = minimum radius of particle
T, T_p = dimensionless gas- and particle-phase temperatures ($T_p \equiv T_p(r_p)$), respectively
V, V_p = dimensionless gas- and particle-phase velocities ($V_p \equiv V_p(r_p)$), respectively
x = dimensionless coordinate along nozzle axis
X_E = dimensionless coordinate at nozzle exit
$\overline{\alpha}$ = film coefficient of heat transfer between gas and particle
γ = gas specific heat ratio
$\hat{\gamma}$ = modified gas specific ratio defined in Eq. (92)
Γ_1, Γ_2, Γ_3 = specified parameters to determine $\hat{\gamma}$ defined in Eqs. (84), (85) and (86), respectively
δ = exponent in the viscosity-temperature Eq. (53)
θ = $\overline{c}_{pp} / \overline{c}_{pg}$
$\overline{\kappa}$ = thermal conductivity of gas
λ = $(2/3)(Pr \cdot \theta)^{-1}$ defined in Eq. (59)
$\overline{\mu}$ = gas viscosity
$\overline{\mu}_0$ = gas viscosity at reservoir state

ν = $(\dot{M}_g / \dot{M}_p)\nu_0$ defined in Eq. (48)

ν_0 = $\overline{R}_{p0} / \overline{\rho}_0$ defined in Eq. (49)

ρ = dimensionless gas density

$\overline{\rho}_{mp}$ = particle material density

ρ_p = dimensionless particle density function ($\rho_p \equiv \rho_p(r_p)$)

ϕ = dimensionless continuous distribution function of particle sizes ($\phi \equiv \phi(r_p)$)

Superscript

$(\bar{\ })$ = dimensioned quantity

Subscript

0 = quantity in reservoir or stagnation state

$*$ = quantity at nozzle throat

E(or e) = quantity at nozzle exit

g = gas-phase

p = particle-phase

1. Introduction

A number of processes in iron- and steelmaking industries positively introduce the utilization of two-phase or multiphase flows. For example, the mist cooling method, which is commonly applied to the secondary cooling zone of continuously cast slabs, is different from other kinds of cooling methods in a few points. First, the mist consists of a two-phase, that is, gas-particle mixtures. Second, the flow pattern in a nozzle varies with the loading ratio, that is, the particle-to-gas mass flow rate ratio. Third, the change in the loading ratio has an appreciable effect on the cooling intensity for the solidified shell. Fourth, the difference in particle size brings on a change in the slip ratio, that is, the ratio of particle velocity to gas velocity, when a continuous distribution of particle size is present.

From such a point of view, the analysis of a two-phase flow in a nozzle is of importance for designing the nozzle to control the mist cooling intensity. However, we suppose that this investigation is not fresh from a historical point of view. This would originate from the development of the propulsive nozzle of the rocket motor[1)~3)].

Zucrow and Hoffman[4)] have described the system of equations governing the steady

quasi-one-dimensional flow of a gas-particle mixture. It consists of a particle continuity euation, a particle momentum equation, a particle energy equation, a particle equation of state, a gas continuity equation, a gas momentum equation, a gas energy equation and a gas equation of state. Then, we have rearranged the above system of equations so that the system gives a fit to the case where particles have a continuous distribution of particle size[5]. This is because it is far more common to consider that particles in a two-phase do not have a single size, but take a continuous distribution of size. Again, the nozzle flow of mist consisting of gas and liquid-particles has been analyzed from a numerical point of view. By so doing, the situation has been premised where a gas containing suspended liquid-particles is initially stored in a relatively large reservoir, and the gas-particle mixture directly flows through a nozzle. However, the reservoir pressure is not allowed to be so high that the gas velocity is beyond the sonic region, because the system of equations described in Ref. (5) is singular in the transonic region.

Thereafter, we have extended the governing equations so that they cover the whole gas velocity regions from the subsonic to the supersonic velocities through the throat of a converging-diverging nozzle[6]. In reality, only the equation to determine the gas velocity has been modified in the form. That is, the equation has been rewritten into the form including the term of pressure profile, instead of the term of the variational nozzle cross-sectional area along the whole nozzle length.

In the present paper, we wish to review the system of equations governing the nozzle flow of gas-particle mixture to evaluate all the flow properties in the flow field. Next, we will examine the numerical treatment of the system of governing equations for the situation where the equation for the determiation of gas-phase velocity is singular in the transonic region. Again, we wish to consider the problem concerning the perturbation procedure between the equilibrium and non-equilibrium flows from a point of view of computational physics. Then, the theoretical model is applied to the case where a gas-particle mixture is composed of air and water-particles in relation to the mist nozzle flow adopted to the secondary cooling zone of continuously cast slabs. The results so obtained are examined and discussed from a numerical point of view.

2. Governing equations

According to Zucrow and Hoffman[4], the theoretical flow model for a gas carrying suspended condensed particles will be constructed on the following assumptions : First, the flow is steady and quasi-one-dimensional, and the mass flow rate for both gas- and particle-phases is conserved in a system. But, the particles occupy negligible volume, that is, the ratio of the gas density to the material density of particles is negligibly

slight. Second, the system of a gas-particle mixture flow in a nozzle does not interact with the external system. That is, it is assumed that there is no external work, no external heat transfer through the nozzle wall, no gravitational effect and no wall friction. Third, the motion of the flowing gas obeys the Euler equation. Namely, the gas is regarded as inviscid apart from the drag force exerted by all of the particles on the gas. Fourth, all of the particles are spherical in shape, incompressible and do not interact with each other. Fifth, the heat transfer between the gas- and partcle-phases is taken into consideration in the form proportional to the temperature difference between gas and particle. But, there is no internal temperature distribution in the radial direction of particles. Also, the gas, as well as the particles, has a constant specific heat.

On the aforementioned premises, the system of governing equations for the nozzle flow of the gas-particle mixture will be derived.

It should previously be remembered that the dimensional quantities are denoted by the overbar, and no overbar denotes the dimensionless quantities throughout the present paper.

First, let us define a continuous distribution function of paricle size as follows;

$$\bar{N}_p\bar{\phi}(\bar{r}_p)=\bar{n}_p(\bar{r}_p)\,;\qquad \bar{\phi}(\bar{r}_p)=\bar{n}_p(\bar{r}_p)\,/\,\bar{N}_p \tag{1}$$

so that the following relation,

$$\int_{\bar{r}_{p,min}}^{\bar{r}_{p,max}}\bar{\phi}(\bar{r}_p)d\bar{r}_p=1 \tag{2}$$

holds true, in which $\bar{r}_{p,min}$ and $\bar{r}_{p,max}$ are the minimum and the maximum radii of the particles contained in the mixture. It is noted that for the indication of the definite integration taken over all sizes in $[\bar{r}_{p,min},\ \bar{r}_{p,max}]$, the lower and upper limits will be omitted for the sake of brevity.

Next, we have

$$\int\frac{4}{3}\pi\bar{r}_p^{\,3}\bar{n}_{p0}(\bar{r}_p)\bar{\rho}_{mp}d\bar{r}_p=\frac{4}{3}\pi\bar{l}_{p0}^{\,3}\bar{N}_{p0}\bar{\rho}_{mp}$$

so that

$$\int\bar{n}_{p0}(\bar{r}_p)\bar{r}_p^{\,3}d\bar{r}_p=\bar{l}_{p0}^{\,3}\bar{N}_{p0}\,;\qquad \int\frac{\bar{n}_{p0}(\bar{r}_p)}{\bar{N}_{p0}}\bar{r}_p^{\,3}d\bar{r}_p=\bar{l}_{p0}^{\,3}$$

Using the relation of $\bar{n}_{p0}(\bar{r}_p)\,/\,\bar{N}_{p0}=\bar{\phi}_0(\bar{r}_p)$ (ref. Eq. (1)), there becomes

$$\bar{l}_{p0}^{\,3}=\int\bar{\phi}_0(\bar{r}_p)\bar{r}_p^{\,3}d\bar{r}_p$$

Therefore,

$$\int\{\bar{l}_{p0}\bar{\phi}_0(\bar{r}_p)\}(\bar{r}_p\,/\,\bar{l}_{p0})^3d(\bar{r}_p\,/\,\bar{l}_{p0})=1$$

or

$$\int\phi_0(r_p)r_p^{\,3}dr_p=1 \tag{3}$$

in which $\bar{r}_p / \bar{l}_{p0} = r_p$ and $\bar{l}_{p0}\bar{\phi}_0(\bar{r}_p) = \phi_0(r_p)$ (4)

Furthermore, it holds true from Eq. (2) that

$$\int \bar{\phi}(\bar{r}_p)d\bar{r}_p = \int \bar{l}_{p0}\bar{\phi}(\bar{r}_p)d\left(\frac{\bar{r}_p}{\bar{l}_{p0}}\right) = \int_{r_{p,min}}^{r_{p,max}} \phi(r_p)dr_p = 1 \tag{5}$$

in which

$$\bar{l}_{p0}\bar{\phi}(\bar{r}_p) = \phi(r_p), \quad r_{p,min} = \bar{r}_{p,min} / \bar{l}_{p0}, \quad r_{p,max} = \bar{r}_{p,max} / \bar{l}_{p0} \tag{6}$$

Here it should be remarked that $\bar{\phi}(\bar{r}_p)$ as well as $\phi(r_p)$ is variable along the nozzle axis, that is, $\bar{\phi}(\bar{x}, \bar{r}_p) \equiv \bar{\phi}(\bar{r}_p)$ and $\phi(x, r_p) \equiv \phi(r_p)$. But, note that the independent variable x is omitted for the simple description.

Second, let us define the dimensionless density function of the particle of r_p in the form of

$$\rho_p(r_p) = \frac{\bar{\rho}_p(\bar{r}_p)\bar{l}_{p0}}{\bar{R}_{p0}} = \frac{\bar{n}_p(\bar{r}_p)(4\pi / 3)\bar{r}_p^3\bar{\rho}_{mp}\bar{l}_{p0}}{\bar{N}_{p0}(4\pi / 3)\bar{l}_{p0}^3\bar{\rho}_{mp}}$$

$$= \frac{\bar{n}_p(\bar{r}_p)\bar{l}_{p0}}{\bar{N}_{p0}} r_p^3 = n_p(r_p)r_p^3 \tag{7}$$

in which $\bar{N}_{p0}$ ($\equiv \bar{N}_{p0}(\bar{x}_0)$) is the total number of particles per unit volume at the reservoir ($\bar{x} = \bar{x}_0$), and

$$n_p(r_p)\ (\equiv n_p(x, r_p)) = \frac{\bar{n}_p(\bar{r}_p)\bar{l}_{p0}}{\bar{N}_{p0}} \qquad (\bar{n}_p(\bar{r}_p) \equiv \bar{n}_p(\bar{x}, \bar{r}_p)) \tag{8}$$

Next, combining Eq. (8) to Eqs. (1) and (2), we have

$$\bar{N}_p\ (\equiv \bar{N}_p(\bar{x})) = \int \bar{n}_p(\bar{r}_p)d\bar{r}_p = \int \frac{n_p(r_p)\bar{N}_{p0}}{\bar{l}_{p0}} d\bar{r}_p$$

$$= \bar{N}_{p0}\int n_p(r_p)dr_p = \bar{N}_{p0}N_p \tag{9}$$

Thereby

$$N_p = \int n_p(r_p)dr_p = \frac{\bar{N}_p}{\bar{N}_{p0}} \quad \text{and} \quad \phi(r_p) = \frac{n_p(r_p)}{N_p} \quad \text{(see Eq. (5))} \tag{10}$$

Now, we consider the system of equations governing the nozzle flow of a two-phase mixture on the dimensional space. First, the particle continuity equation is given by

$$\dot{\bar{m}}_p(\bar{x}, \bar{r}_p) = \bar{\rho}_p(\bar{x}, \bar{r}_p)\bar{A}(\bar{x})\bar{V}_p(\bar{x}, \bar{r}_p)$$

Unless otherwise provided, the variable x will be omitted from now on as follows;

$$\dot{\bar{m}}_p(\bar{r}_p) = \bar{\rho}_p(\bar{r}_p)\bar{A}\bar{V}_p(\bar{r}_p)$$

$$= \bar{n}_p(\bar{r}_p)(4\pi / 3)\bar{r}_p^3\bar{\rho}_{mp}\bar{A}\bar{V}_p(\bar{r}_p) = \text{const.} \tag{11}$$

Again,

$$\bar{M}_p=\int \bar{m}_p(\bar{r}_p)d\bar{r}_p \tag{12}$$

Next, the particle momentum equation for a particle of $\bar{r}_p$ yields

$$\frac{4}{3}\pi\bar{r}_p^3\bar{\rho}_{mp}\bar{V}_p(\bar{r}_p)\frac{d}{d\bar{x}}\bar{V}_p(\bar{r}_p)=C_D\frac{1}{2}\pi\bar{r}_p^2\bar{\rho}[\bar{V}-\bar{V}_p(\bar{r}_p)]|\bar{V}-\bar{V}_p(\bar{r}_p)| \tag{13}$$

so that

$$\bar{V}_p(\bar{r}_p)\frac{d}{d\bar{x}}\bar{V}_p(\bar{r}_p)=\frac{(3/8)\bar{\rho}C_D}{\bar{\rho}_{mp}\bar{r}_p}[\bar{V}-\bar{V}_p(\bar{r}_p)]|\bar{V}-\bar{V}_p(\bar{r}_p)| \tag{14}$$

In the Stockes flow regime, the drag coefficient is expressed as

$$C_{D,Stokes}=\frac{24}{Re_p}=\frac{24\bar{\mu}}{(2\bar{r}_p)\bar{\rho}|\bar{V}-\bar{V}_p(\bar{r}_p)|} \tag{15}$$

By definition, we put

$$f_p\equiv\frac{C_D}{C_{D,Stokes}}=\frac{C_D(2\bar{r}_p)\bar{\rho}|\bar{V}-\bar{V}_p(\bar{r}_p)|}{24\bar{\mu}} \tag{16}$$

Then, combining Eqs. (14) and (16), we have

$$\bar{V}_p(\bar{r}_p)\frac{d}{d\bar{x}}\bar{V}_p(\bar{r}_p)=\frac{(9/2)\bar{\mu}f_p}{\bar{\rho}_{mp}\bar{r}_p^2}[\bar{V}-\bar{V}_p(\bar{r}_p)] \tag{17}$$

The particle energy equaion for a particle of $\bar{r}_p$ is given by

$$\frac{4}{3}\pi\bar{r}_p^3\bar{\rho}_{mp}\bar{V}_p(\bar{r}_p)\frac{d}{d\bar{x}}\bar{h}_p(\bar{r}_p)=\bar{\alpha}(4\pi\bar{r}_p^2)[\bar{T}-\bar{T}_p(\bar{r}_p)] \tag{18}$$

The film coefficient $\bar{\alpha}$ is defined in term of the Nusselt number Nu. That is,

$$Nu=\frac{\bar{\alpha}(2\bar{r}_p)}{\bar{\kappa}} \tag{19}$$

Again, the Prandtl number is defined by

$$Pr=\frac{\bar{C}_{pg}\bar{\mu}}{\bar{\kappa}} \tag{20}$$

In the Stokes flow regime, $Nu_{Stokes}=2$. By definition, let

$$g_p=\frac{Nu}{Nu_{Stokes}}=\frac{Nu}{2} \tag{21}$$

Combining Egs. (19) ~ (21), we have

$$\bar{\alpha}=\frac{g_p\bar{C}_{pg}\bar{\mu}}{\bar{r}_pPr} \tag{22}$$

Substituting Eq. (22) into Eq. (18) yields

$$\bar{V}_p(\bar{r}_p)\frac{d}{d\bar{x}}\bar{h}_p(\bar{r}_p)=\frac{3g_p\bar{C}_{pg}\bar{\mu}}{\bar{\rho}_{mp}\bar{r}_p^2Pr}[\bar{T}-\bar{T}_p(\bar{r}_p)] \tag{23}$$

Here, introducing the particle equation of state,

$$\bar{h}_p(\bar{r}_p)=\bar{c}_{pp}\bar{T}_p(\bar{r}_p) \tag{24}$$

to Eq. (23), we have

$$\bar{V}_p(\bar{r}_p)\frac{d}{d\bar{x}}\bar{T}_p(\bar{r}_p)=\frac{3g_p\bar{c}_{pg}\bar{\mu}}{\bar{\rho}_{mp}\bar{r}_p^2\bar{c}_{pp}Pr}[\bar{T}-\bar{T}_p(\bar{r}_p)] \tag{25}$$

Now, let us derive the total drag force $\delta\bar{D}$ exerted by all of the particles on the gas inside of the control volume $(\bar{A}\,d\bar{x})$. For a particle of $\bar{r}_p$, Newton's second law yields

$$\bar{\sigma}_p(\bar{r}_p)\bar{V}_p(\bar{r}_p)\frac{d}{d\bar{x}}\bar{V}_p(\bar{r}_p)=\delta\bar{D}_p(\bar{r}_p) \tag{26}$$

where $\bar{\sigma}_p(\bar{r}_p)$ is the mass of a particle of $\bar{r}_p$ and $\delta\bar{D}_p(\bar{r}_p)$ is the drag force on the particle. Therefore, $\delta\bar{D}$ is given by

$$\delta\bar{D}=\int\frac{\delta\bar{D}_p(\bar{r}_p)}{\bar{\sigma}_p(\bar{r}_p)}[\bar{\rho}_p(\bar{r}_p)\bar{A}d\bar{x}]d\bar{r}_p$$

It follows from Eq. (26) that

$$\frac{\delta\bar{D}}{\bar{A}d\bar{x}}=\int\bar{\rho}_p(\bar{r}_p)\bar{V}_p(\bar{r}_p)\frac{d}{d\bar{x}}\bar{V}_p(\bar{r}_p)d\bar{r}_p \tag{27}$$

Here, it should be noted that $\delta\bar{D}\,/\,(\bar{A}d\bar{x})$ is the total drag force per unit volume.

Next, let us seek the total heat transfer rate $\delta\bar{\dot{Q}}$ for all of the particles per unit mass of the gas inside of $(\bar{A}d\bar{x})$. The heat transfer $\delta\bar{\dot{Q}}_p(\bar{r}_p)$ between the gas and the particle of $\bar{r}_p$ per unit time is given by

$$\delta\bar{\dot{Q}}_p(\bar{r}_p)=\bar{\sigma}_p(\bar{r}_p)\bar{V}_p(\bar{r}_p)\frac{d}{d\bar{x}}\bar{h}_p(\bar{r}_p) \tag{28}$$

Hence,

$$\delta\bar{\dot{Q}}[\bar{\rho}(\bar{A}d\bar{x})]-\int\frac{\delta\bar{\dot{Q}}_p(\bar{r}_p)}{\bar{\sigma}_p(\bar{r}_p)}[\bar{\rho}_p(\bar{r}_p)(\bar{A}d\bar{x})]d\bar{r}_p=0$$

Substituting Eq. (28) into the above equation yields

$$\bar{\rho}\delta\bar{\dot{Q}}=\int\bar{\rho}_p(\bar{r}_p)\bar{V}_p(\bar{r}_p)\frac{d}{d\bar{x}}\bar{h}_p(\bar{r}_p)d\bar{r}_p \tag{29}$$

Here, it should be noted that $\bar{\rho}\delta\bar{\dot{Q}}$ is the energy per unit volume and per unit time.

Again, all of the work expended on the particles by the gas presents itself in the form of an increase in the kinetic energy. So that, for a particle of $\bar{r}_p$

$$\delta\bar{\dot{W}}_p(\bar{r}_p)=\bar{\sigma}_p(\bar{r}_p)\bar{V}_p(\bar{r}_p)\frac{d}{d\bar{x}}\left\{\frac{1}{2}\bar{V}_p^2(\bar{r}_p)\right\} \tag{30}$$

Accordingly,

$$\delta\dot{\bar{W}}[\bar{\rho}(\bar{A}d\bar{x})]-\int\frac{\delta\dot{\bar{W}}_p(\bar{r}_p)}{\bar{\sigma}_p(\bar{r}_p)}[\bar{\rho}_p(\bar{r}_p)(\bar{A}d\bar{x})]d\bar{r}_p=0$$

Substituting Eq. (30) into the above equation, we obtain

$$\bar{\rho}\delta\dot{\bar{W}}=\int\bar{\rho}_p(\bar{r}_p)\bar{V}_p(\bar{r}_p)\frac{d}{d\bar{x}}\left\{\frac{1}{2}\bar{V}_p^2(\bar{r}_p)\right\}d\bar{r}_p=\int\bar{\rho}_p(\bar{r}_p)\bar{V}_p^2(\bar{r}_p)\frac{d}{d\bar{x}}\bar{V}_p(\bar{r}_p)d\bar{r}_p \tag{31}$$

We will now turn to a review of the equations governing the gas-phase. The gas continuity equation is clearly given by

$$\dot{\bar{M}}_g=\bar{\rho}\bar{A}\bar{V}=\text{const.}\quad(\bar{\rho}=\bar{\rho}(\bar{x}),\ \bar{V}=\bar{V}(\bar{x})) \tag{32}$$

or

$$\frac{1}{\bar{\rho}}\frac{d\bar{\rho}}{d\bar{x}}+\frac{1}{\bar{A}}\frac{d\bar{A}}{d\bar{x}}+\frac{1}{\bar{V}}\frac{d\bar{V}}{d\bar{x}}=0 \tag{33}$$

The gas momentum equation is obtained by taking into consideration the total drag force per unit volume as follows:

$$\bar{\rho}\bar{V}\frac{d\bar{V}}{d\bar{x}}=-\frac{d\bar{p}}{d\bar{x}}-\frac{\delta\bar{D}}{\bar{A}d\bar{x}} \tag{34}$$

This is the Euler equation with the drag force term as the body force. Using Eq. (27), Eq. (34) becomes

$$\bar{\rho}\bar{V}\frac{d\bar{V}}{d\bar{x}}+\int\bar{\rho}_p(\bar{r}_p)\bar{V}_p(\bar{r}_p)\frac{d}{d\bar{x}}\bar{V}_p(\bar{r}_p)d\bar{r}_p+\frac{d\bar{p}}{d\bar{x}}=0 \tag{35}$$

Next, it holds true that

$$\delta\bar{W}+\delta\bar{Q}+d\bar{h}+\bar{V}d\bar{V}=0 \tag{36}$$

in which $\delta\bar{W}$ is the work per unit mass done by the gas on all of the particles, due to the drag force, and $\delta\bar{Q}$ is the heat per unit mass transferred from the gas to all of the particles. The expression of Eq. (36) may be converted into a rate basis. Thus,

$$\delta\dot{\bar{W}}+\delta\dot{\bar{Q}}+\frac{d\bar{h}}{d\bar{t}}+\bar{V}\frac{d\bar{V}}{d\bar{t}}=\delta\dot{\bar{W}}+\delta\dot{\bar{Q}}+\bar{V}\frac{d\bar{h}}{d\bar{x}}+\bar{V}^2\frac{d\bar{V}}{d\bar{x}}=0 \tag{37}$$

Substituting Eq. (29) and Eq. (31) into the above relation yields

$$\bar{\rho}\bar{V}\frac{d\bar{h}}{d\bar{x}}+\bar{\rho}\bar{V}^2\frac{d\bar{V}}{d\bar{x}}+\int\bar{\rho}_p(\bar{r}_p)\bar{V}_p(\bar{r}_p)\frac{d}{d\bar{x}}\bar{h}_p(\bar{r}_p)d\bar{r}_p+\int\bar{\rho}_p(\bar{r}_p)\bar{V}_p^2(\bar{r}_p)\frac{d}{d\bar{x}}\bar{V}_p(\bar{r}_p)d\bar{r}_p=0 \tag{38}$$

or

$$\frac{d\bar{h}}{d\bar{x}}+\bar{V}\frac{d\bar{V}}{d\bar{x}}+\int\frac{\bar{\rho}_p(\bar{r}_p)\bar{V}_p(\bar{r}_p)}{\bar{\rho}\bar{V}}\frac{d}{d\bar{x}}\bar{h}_p(\bar{r}_p)d\bar{r}_p$$

$$+\int\frac{\bar{\rho}_p(\bar{r}_p)\bar{V}_p(\bar{r}_p)}{\bar{\rho}\bar{V}}\bar{V}_p(\bar{r}_p)\frac{d}{d\bar{x}}\bar{V}_p(\bar{r}_p)d\bar{r}_p=0 \tag{39}$$

Substituting Eq. (11) and Eq. (32) into Eq. (39), we obtain

$$\frac{d\bar{h}}{d\bar{x}}+\bar{V}\frac{d\bar{V}}{d\bar{x}}+\int\frac{\dot{\bar{m}}_p(\bar{r}_p)}{\dot{\bar{M}}_g}\frac{d}{d\bar{x}}\bar{h}_p(\bar{r}_p)d\bar{r}_p+\int\frac{\dot{\bar{m}}_p(\bar{r}_p)}{\dot{\bar{M}}_g}\bar{V}_p(\bar{r}_p)\frac{d}{d\bar{x}}\bar{V}_p(\bar{r}_p)d\bar{r}_p=0 \tag{40}$$

Integrating the aforementioned with respect to x, we have

$$\bar{h}+\frac{1}{2}\bar{V}^2+\int\frac{\dot{\bar{m}}_p(\bar{r}_p)}{\dot{\bar{M}}_g}\bar{h}_p(\bar{r}_p)d\bar{r}_p+\int\frac{\dot{\bar{m}}_p(\bar{r}_p)}{\dot{\bar{M}}_g}\frac{1}{2}\bar{V}_p{}^2(\bar{r}_p)d\bar{r}_p=\text{const.} \tag{41}$$

or

$$\bar{h}+\frac{1}{2}\bar{V}^2+\int\frac{\dot{\bar{m}}_p(\bar{r}_p)}{\dot{\bar{M}}_g}[\bar{h}_p(\bar{r}_p)+\frac{1}{2}\bar{V}^2(\bar{r}_p)]d\bar{r}_p=\bar{H}+\int\frac{\dot{\bar{m}}_p(\bar{r}_p)}{\dot{\bar{M}}_g}\bar{H}_p(\bar{r}_p)d\bar{r}_p \tag{42}$$

Finally, the gas equation of state is given by

$$d\bar{h}=\bar{c}_{pg}d\bar{T} \tag{43}$$

$$\bar{p}=\bar{\rho}\bar{R}\bar{T} \tag{44}$$

Up to this point we have completed the system of equations governing the nozzle flow of gas-particle mixtures on the dimensional space. Here, we wish to stress that in our calculation, the dimensionless parameters are adopted, and the governing equations to be solved will be expressed by dimensionless quantities. It is physically important to rewrite the dimensional equations into the dimensionless ones and solve them as to the similarity of the flow pattern as well as the general validity.

The main dimensionless variables introduced into the system of governing equations are defined as

$$\bar{x}/\bar{L}_*=x,\ \bar{A}/\bar{A}_*=A,\ \bar{\rho}/\bar{\rho}_0=\rho,\ \bar{p}/\bar{p}_0=p,$$
$$\bar{V}/\bar{a}_0=V,\ \bar{V}_p/\bar{a}_0=V_p,\ \bar{T}/\bar{T}_0=T,\ \bar{T}_p/\bar{T}_0=T_p \tag{45}$$

where $\bar{\rho}\equiv\bar{\rho}(\bar{x})$, $\rho\equiv\rho(x)$, $\bar{p}\equiv\bar{p}(\bar{x})$, $p\equiv p(x)$, $\bar{V}\equiv\bar{V}(\bar{x})$, $V\equiv V(x)$, $\bar{V}_p\equiv\bar{V}_p(\bar{x},\ \bar{r}_p)$, $V_p\equiv V_p(x,\ r_p)$, $\bar{T}\equiv\bar{T}(\bar{x})$, $T\equiv T(x)$, $\bar{T}_p\equiv\bar{T}_p(\bar{x},\ \bar{r}_p)$ and $T_p\equiv T_p(x,\ r_p)$. However, as mentioned previously, the independent variable x as well as $\bar{x}$ is omitted, for example, the variables such as $V(x)$, $V_p(x,\ r_p)$ will be abbreviated to V, $V_p(r_p)$.

Next, let us define the dimensionless mass flow rate for the gas-phase and the particle-phase as

$$\dot{M}_g=\frac{\dot{\bar{M}}_g}{\bar{\rho}_0\bar{a}_0\bar{A}_*} \tag{46}$$

$$\dot{M}_p=\frac{\dot{\bar{M}}_p}{\bar{R}_{p0}\bar{a}_0\bar{A}_*} \tag{47}$$

Thus, the loading radio is given by

$$\nu=\frac{\bar{\dot{M}}_p}{\bar{\dot{M}}_g}=\frac{\dot{M}_p}{\dot{M}_g}\frac{\bar{R}_{p0}}{\bar{\rho}_0}=\frac{\dot{M}_p}{\dot{M}_g}\nu_0 \tag{48}$$

$$\nu_0=\frac{\bar{R}_{p0}}{\bar{\rho}_0} \tag{49}$$

Now, let us rewrite the system of equations by introducing dimensionless quantities.

i) Particle continuity equation

Combining Eqs. (7), (11) and (45), we obtain

$$\bar{\dot{m}}_p(\bar{r}_p)=(\rho_p(r_p)\bar{R}_{p0}/\bar{l}_{p0})\bar{A}_*A\bar{a}_0V_p(r_p)$$

Hence,

$$\dot{m}_p(r_p)=\rho_p(r_p)AV_p(r_p)=\frac{\bar{\dot{m}}_p(\bar{r}_p)\bar{l}_{p0}}{\bar{R}_{p0}\bar{A}_*\bar{a}_0} \tag{50}$$

and

$$\bar{\dot{M}}_p=\int\bar{\dot{m}}_p(\bar{r}_p)d\bar{r}_p=\bar{R}_{p0}\bar{a}_0\bar{A}_*\int\rho_p(r_p)AV_p(r_p)dr_p$$

so that

$$\dot{M}_p=\int\dot{m}_p(r_p)dr_p=\int\rho_p(r_p)AV_p(r_p)dr_p=\frac{\bar{\dot{M}}_p}{\bar{R}_{p0}\bar{a}_0\bar{A}_*} \tag{51}$$

Note that Eq. (51) agrees with $\dot{M}_p$ defined by Eq. (47).

ii) Particle momentum equation

Substituting Eq. (4) and Eq. (45) into Eq. (17) and arranging the form, we have

$$V_p(r_p)\frac{d}{dx}V_p(r_p)=\left(\frac{9}{2}\cdot\frac{\bar{\mu}\bar{L}_*}{\bar{\rho}_{mp}\bar{l}_{p0}^2\bar{a}_0}\right)\frac{f_p}{r_p^2}[V-V_p(r_p)] \tag{52}$$

Here, the gas viscosity $\bar{\mu}$ is commonly given by

$$\bar{\mu}=\bar{\mu}_0(\bar{T}/\bar{T}_0)^\sigma=\bar{\mu}_0T^\sigma \tag{53}$$

where δ is a constant. Thus, Eq. (52) becomes

$$V_p(r_p)\frac{d}{dx}V_p(r_p)=A_{p0}f_p\frac{T^\sigma}{r_p^2}[V-V_p(r_p)] \tag{54}$$

where

$$A_{p0}=\frac{9}{2}\cdot\frac{\bar{\mu}_0\bar{L}_*}{\bar{\rho}_{mp}\bar{l}_{p0}^2\bar{a}_0} \tag{55}$$

Again, f_p, defined by Eq. (16), is concerned with C_D, and $C_{D,Stokes}$. C_D is determined by

the Henderson correlating equation[7], and $C_{D,Stokes}=24/Re_p$ is the Stokes law of drag coefficient for sphere, as formulated in Eq. (15). In this case, the particle Reynolds number is based upon the relative velocity $|\bar{V}-\bar{V}_p(\bar{r}_p)|$, the particle diameter $2\bar{r}_p$ and the gas viscosity given by Eq. (53), and defined by

$$Re_p=\frac{(2\bar{r}_p)|\bar{V}-\bar{V}_p(\bar{r}_p)|\bar{\rho}}{\bar{\mu}}=Re_{p0}\frac{r_p|V-V_p(r_p)|}{T^\sigma/\rho}$$

with

$$Re_{p0}=\frac{2\bar{l}_{p0}\bar{a}_0}{\bar{\mu}_0/\bar{\rho}_0} \qquad (56)$$

iii) Particle energy equation

See Eq. (25). Substituting Eqs. (4), (45) and (53) into Eq. (25) yields

$$V_p(r_p)\frac{d}{dx}T_p(r_p)=\left(\frac{3\bar{\mu}_0\bar{c}_{pg}\bar{L}_*}{Pr\bar{l}_{p0}^2\bar{c}_{pp}\bar{\rho}_{mp}\bar{a}_0}\right)g_p\frac{T^\sigma}{r_p^2}[T-T_p(r_p)] \qquad (57)$$

in which put

$$\frac{3\bar{\mu}_0\bar{c}_{pg}\bar{L}_*}{Pr\bar{l}_{p0}^2\bar{c}_{pp}\bar{\rho}_{mp}\bar{a}_0}=\left(\frac{9}{2}\cdot\frac{\bar{\mu}_0\bar{L}_*}{\bar{\rho}_{mp}\bar{l}_{p0}^2\bar{a}_0}\right)\left(\frac{2}{3}\cdot\frac{1}{Pr\theta}\right)=\lambda A_{p0} \qquad (58)$$

where

$$\theta=\frac{\bar{c}_{pp}}{\bar{c}_{pg}} \quad \text{and} \quad \lambda=\frac{2}{3}\frac{1}{Pr\theta} \qquad (59)$$

Hence,

$$V_p(r_p)\frac{d}{dx}T_p(r_p)=\lambda A_{p0}g_p\frac{T^\sigma}{r_p^2}[T-T_p(r_p)] \qquad (60)$$

in which $g_p=Nu/2$, as defined in Eq. (21). For the particle Nusselt number Nu, the empirical expression by Carlson and Hoglund[8] is adopted in our numerical experiments.

In passing, it should be noted that the particle equation of state has been coupled with the particle energy equation (see Eqs. (24) and (25)).

iv) Gas continuity equation (see Eq. (32))

$$\bar{M}_g=\bar{\rho}\bar{A}\bar{V}=\bar{\rho}_0\rho\bar{A}_*A\bar{a}_0V$$

Thus,

$$\dot{M}_g=\rho AV=\frac{\bar{M}_g}{\bar{\rho}_0\bar{a}_0\bar{A}_*} \qquad (61)$$

Note that Eq. (61) agrees with $\dot{M}_g$ defined by Eq. (46).

v) Gas momentum equation

Combining Eqs. (7), (35), (45) and (49), we obtain

$$\rho V\frac{dV}{dx}+\nu_0\int\rho_p(r_p)V_p(r_p)\frac{d}{dx}V_p(r_p)dr_p+\frac{\bar{p}_0}{\bar{\rho}_0\bar{a}_0^2}\frac{dp}{dx}=0 \tag{62}$$

Here, $\bar{p}_0=\bar{\rho}_0\bar{R}\bar{T}_0$ and $\bar{a}_0^2=\gamma\bar{R}\bar{T}_0$, so that $\bar{p}_0/(\bar{\rho}_0\bar{a}_0^2)=1/\gamma$.

Eq. (62) results in

$$\rho V\frac{dV}{dx}+\nu_0\int\rho_p(r_p)V_p(r_p)\frac{d}{dx}V_p(r_p)dr_p+\frac{1}{\gamma}\frac{dp}{dx}=0 \tag{63}$$

vi) Gas energy equation

Substituting Eqs. (4), (7), (43), (45), (49) and (59) into Eq. (38) and arranging the form, we have

$$\rho V\frac{dT}{dx}+\frac{\bar{a}_0^2}{\bar{c}_{pg}\bar{T}_0}\rho V^2\frac{dV}{dx}+\theta\nu_0\int\rho_p(r_p)V_p(r_p)\frac{d}{dx}T_p(r_p)dr_p$$
$$+\frac{\bar{a}_0^2}{\bar{c}_{pg}\bar{T}_0}\nu_0\int\rho_p(r_p)V_p^2(r_p)\frac{d}{dx}V_p(r_p)dr_p=0 \tag{64}$$

Because $\bar{c}_{pg}=\gamma\bar{R}/(\gamma-1)$, $\bar{a}_0^2/(\bar{c}_{pg}\bar{T}_0)=\gamma-1$, Eq. (64) becomes

$$\frac{dT}{dx}+(\gamma-1)V\frac{dV}{dx}+\theta\nu_0\int\frac{\rho_p(r_p)V_p(r_p)}{\rho V}\frac{d}{dx}T_p(r_p)dr_p$$
$$+(\gamma-1)\nu_0\int\frac{\rho_p(r_p)V_p(r_p)}{\rho V}V_p(r_p)\frac{d}{dx}V_p(r_p)dr_p=0$$

Noting that $\rho_p(r_p)V_p(r_p)/(\rho V)=\dot{m}_p(r_p)/\dot{M}_g$, thus,

$$\frac{dT}{dx}+(\gamma-1)V\frac{dV}{dx}+\theta\nu_0\int\frac{\dot{m}_p(r_p)}{\dot{M}_g}\frac{d}{dx}T_p(r_p)dr_p$$
$$+(\gamma-1)\nu_0\int\frac{\dot{m}_p(r_p)}{\dot{M}_g}V_p(r_p)\frac{d}{dx}V_p(r_p)dr_p=0 \tag{65}$$

Integrating the above equation with respect to x and noting that

$$\int\frac{\dot{m}_p(r_p)}{\dot{M}_g}dr_p=\frac{\dot{M}_p}{\dot{M}_g}=\frac{\nu}{\nu_0}\quad\text{(see Eq. (48))} \tag{66}$$

we have

$$T+\frac{1}{2}(\gamma-1)V^2+\nu_0\int\frac{\dot{m}_p(r_p)}{\dot{M}_g}\left[\theta T_p(r_p)+\frac{1}{2}(\gamma-1)V_p^2(r_p)\right]dr_p=1+\nu\theta \tag{67}$$

vii) Gas equation of state

It is self-evident from Eqs. (44) and (45) that

$$p=\rho T \tag{68}$$

viii) Sonic speed and Mach number

$$a=\frac{\bar{a}}{\bar{a}_0}=\sqrt{\frac{\bar{T}}{\bar{T}_0}}=\sqrt{T} \tag{69}$$

$$M=\frac{\bar{V}}{\bar{a}}=\frac{\bar{a}_0 V}{\bar{a}_0 a}=\frac{V}{a}=\frac{V}{\sqrt{T}} \tag{70}$$

ix) Equation for determining the gas velocity V

Substituting $V_p(r_p)dV_p(r_p)/dx$ and $dT_p(r_p)/dx$ appearing in Eqs. (54) and (60), respectively, into Eq. (65), and expressing dV/dx explicity, we have

$$\frac{dV}{dx}=-\frac{1}{(\gamma-1)V}\left[\frac{dT}{dx}+\nu_0\int\frac{\dot{m}_p(r_p)}{\dot{M}_g}\left\{\theta\lambda A_{p0}g_p\frac{T^\sigma}{r_p^2}\frac{[T-T_p(r_p)]}{V_p(r_p)}\right.\right.$$
$$\left.\left.+(\gamma-1)A_{p0}f_p\frac{T^\sigma}{r_p^2}[V-V_p(r_p)]\right\}dr_p\right] \tag{71}$$

On the other hand, from the gas equation of state (see Eq. (68)), we have

$$\frac{dT}{dx}=\frac{d}{dx}\frac{p}{\rho}=T\left(\frac{1}{p}\frac{dp}{dx}-\frac{1}{\rho}\frac{d\rho}{dx}\right) \tag{72}$$

Substituting $V_p(r_p)dV_p(r_p)/dx$ appearing in Eq. (54) into Eq. (63), we obtain

$$\frac{dp}{dx}=-\gamma\left[\rho V\frac{dV}{dx}+\nu_0\int\rho_p(r_p)A_{p0}f_p\frac{T^\sigma}{r_p^2}[V-V_p(r_p)]dr_p\right] \tag{73}$$

Again, Eq. (61) corresponds to

$$\frac{1}{\rho}\frac{d\rho}{dx}=-\frac{1}{A}\frac{dA}{dx}-\frac{1}{V}\frac{dV}{dx} \tag{74}$$

Substituting Eqs. (73) and (74) into Eq. (72) gives

$$\frac{dT}{dx}=T\left[\left(\frac{1}{V}-\frac{\gamma V}{T}\right)\frac{dV}{dx}+\frac{1}{A}\frac{dA}{dx}\right.$$
$$\left.-\frac{\gamma\nu_0}{p}\int\rho_p(r_p)A_{p0}f_p\frac{T^\sigma}{r_p^2}[V-V_p(r_p)]dr_p\right] \tag{75}$$

Substituting Eq. (75) into Eq. (71) and arranging the form of equation to express dV/dx explicitly yields

$$\frac{dV}{dx}=-\frac{M^2}{1-M^2}\frac{1}{V}\left[\frac{T}{A}\frac{dA}{dx}-\gamma\nu_0A_{p0}\frac{T^\sigma}{\rho}\int\rho_p(r_p)\frac{f_p}{r_p^2}[V-V_p(r_p)]dr_p\right.$$
$$+\nu_0A_{p0}T^\sigma\int\frac{\dot{m}_p(r_p)}{\dot{M}_g}\left\{\theta\lambda\frac{g_p}{r_p^2}\frac{T-T_p(r_p)}{V_p(r_p)}\right.$$
$$\left.\left.+(\gamma-1)\frac{f_p}{r_p^2}[V-V_p(r_p)]\right\}dr_p\right] \tag{76}$$

At a glance, the above equation is singular in the transonic region. Therefore, this is not applicable to the case where the gas velocity is beyond the sonic region from a numeri-

cal standpoint.

Then, let us combine the particle momentum equation (54) and the gas momentum equation (63). Thus, we obtain

$$\frac{dV}{dx}=-\frac{1}{\rho V\gamma}\frac{dp}{dx}-\frac{A_{p0}}{\rho V}\nu_0 T^{\sigma}\int\rho_p(r_p)f_p\frac{V-V_p(r_p)}{r_p^2}dr_p \tag{77}$$

This equation involves the term concerning the pressure profile along the nozzle axis. Therefore, if the pressure profile, in advance, is given over the whole length of the nozzle axis, the cross-sectional area along the nozzle axis is uniquely determinable in accord with the given pressure profile.

According to Zucrow and Hoffman, the determination method of V by Eq. (76) will be called the specified area method, and that by Eq. (77) will be termed the specified pressure method.

3. Numerical procedure

Among the equations presented in the previous section, Eqs. (50), (54), (60), (61), (63), (67) and (68) comprise a set of seven equations for determining the seven flow properties p, ρ, T, V, $\rho_p(r_p)$, $V_p(r_p)$ and $T_p(r_p)$. Those equations should be combined in a form appropriate for seeking a numerical solution.

However, the creation of the initial condition is very tedious at the start of the numerical calculation. For example, suppose that a gas containing suspended liquid-particles is initially stored in an appreciably large reservoir, and that the gas-particle mixture directly flows through a nozzle. It is common to consider that at the reservoir the gas velocity, as wel as particle velocity, is zero. Thus, the initial situation corresponds to the assumption that the sectional area of the nozzle is infinite at its entrance. It remains to know how the numerical treatment should be made at the initial computational step. Then, let it be assumed that all the particles are in velocity and thermal equilibrium with the gas only near the reservoir. Then the gas, as well as all the particles, may take a non-zero velocity at the entrance of the non-equilibrium region. By so doing, the non-equilibrium flow can be treated as a perturbation from an equilibrium reference flow.

Therefore, we wish to describe the problem of the constant lag flow. Let us now define the following two lag factors,

$$K_p(r_p)=\frac{\overline{V}_p(\overline{r}_p)}{\overline{V}}=\frac{V_p(r_p)}{V} \tag{78}$$

$$L_p(r_p)=\frac{\overline{T}_0-\overline{T}_p(\overline{r}_p)}{\overline{T}_0-\overline{T}}=\frac{1-T_p(r_p)}{1-T} \tag{79}$$

Here, $[1-K_p(r_p)]$ and $[1-L_p(r_p)]$ are called the velocity lag and the thermal lag, respectively. Again, the relation between $K_p(r_p)$ and $L_p(r_p)$,

$$L_p(r_p)=\left(1+3\theta Pr\frac{1-K_p(r_p)}{K_p(r_p)}\right)^{-1} \tag{80}$$

holds true on the assumption that the particle remains in the liquid phase, that $\bar{c}_{pg}$ and $\bar{c}_{pp}$ are constant, and that the velocity lag as well as the thermal lag is constant.

Dividing Eq. (63) by ρV, noting that $\rho_p(r_p)V_p(r_p)/(\rho V)=\dot{m}_p(r_p)/\dot{M}_g$ and that $dV_p(r_p)/dx=K_p(r_p)dV/dx$ by introducing Eq. (78) and rearranging the result, we obtain

$$\gamma\left\{1+\nu_0\int\frac{\dot{m}_p(r_p)}{\dot{M}_g}K_p(r_p)dr_p\right\}V\frac{dV}{dx}+\frac{1}{\rho}\frac{dp}{dx}=0 \tag{81}$$

Next, substituting Eq. (78) and Eq. (79) into Eq. (67) and noting the relation of Eq. (66), we have

$$T\left\{1+\nu_0\theta\int\frac{\dot{m}_p(r_p)}{\dot{M}_g}L_p(r_p)dr_p\right\}+\frac{(\gamma-1)}{2}V^2\left\{1+\nu_0\int\frac{\dot{m}_p(r_p)}{\dot{M}_g}K_p^2(r_p)dr_p\right\}$$
$$=1+\nu_0\theta\int\frac{\dot{m}_p(r_p)}{\dot{M}_g}L_p(r_p)dr_p \tag{82}$$

or

$$\left\{1+\nu_0\theta\int\frac{\dot{m}_p(r_p)}{\dot{M}_g}L_p(r_p)dr_p\right\}\frac{dT}{dx}$$
$$+(\gamma-1)\left\{1+\nu_0\int\frac{\dot{m}_p(r_p)}{\dot{M}_g}K_p^2(r_p)dr_p\right\}V\frac{dV}{dx}=0 \tag{83}$$

Here, we put

$$\Gamma_1=\nu_0\int\frac{\dot{m}_p(r_p)}{\dot{M}_g}K_p(r_p)dr_p \tag{84}$$

$$\Gamma_2=\nu_0\int\frac{\dot{m}_p(r_p)}{\dot{M}_g}K_p^2(r_p)dr_p \tag{85}$$

$$\Gamma_3=\nu_0\theta\int\frac{\dot{m}_p(r_p)}{\dot{M}_g}L_p(r_p)dr_p \tag{86}$$

Thus, Eqs. (81) and (83) can be rewritten into

$$\gamma(1+\Gamma_1)V\frac{dV}{dx}+\frac{1}{\rho}\frac{dp}{dx}=0 \tag{87}$$

$$(1+\Gamma_3)\frac{dT}{dx}+(\gamma-1)(1+\Gamma_2)V\frac{dV}{dx}=0 \tag{88}$$

Using the relation $p=\rho T$, one has

$$\frac{dT}{dx}=\frac{p}{\rho}\left(\frac{1}{p}\frac{dp}{dx}-\frac{1}{\rho}\frac{d\rho}{dx}\right) \tag{89}$$

Substituting VdV/dx appearing in Eq. (87) and dT/dx in Eq. (89) into Eq. (88), we obtain

$$\frac{1}{p}\frac{dp}{dx}-\frac{\gamma(1+\Gamma_1)(1+\Gamma_3)}{\gamma(1+\Gamma_1)(1+\Gamma_3)-(\gamma-1)(1+\Gamma_2)}\frac{1}{\rho}\frac{d\rho}{dx}=0 \tag{90}$$

Hence,

$$p\rho^{-\hat{\gamma}}=p_0\rho_0^{-\hat{\gamma}}=1 \tag{91}$$

in which

$$\hat{\gamma}=\frac{\gamma(1+\Gamma_1)(1+\Gamma_3)}{\gamma(1+\Gamma_1)(1+\Gamma_3)-(\gamma-1)(1+\Gamma_2)} \tag{92}$$

Next, we consider Γ_1, Γ_2 and Γ_3

$$\Gamma_1=\nu_0\int\frac{\dot{m}_p(r_p)}{\dot{M}_g}K_p(r_p)dr_p=\nu_0\int\frac{\rho_p(r_p)AV_p(r_p)}{\rho AV}K_p(r_p)dr_p$$

$$=\frac{\nu_0}{\rho}\int\rho_p(r_p)K_p^2(r_p)dr_p \quad \text{(see Eq. (78))} \tag{93}$$

Here, introducing Eqs. (7) and (10) into the above equation, we have

$$\Gamma_1=\frac{\nu_0}{\rho}\int n_p(r_p)r_p^3K_p^2(r_p)dr_p=\frac{\nu_0N_p}{\rho}\int\phi(r_p)r_p^3K_p^2(r_p)dr_p \tag{94}$$

This is determined by a perturbation from a reservoir condition. That is, $N_p\to N_{p0}\ (=1)$, $\rho\to 1$ and $\phi(r_p)\to\phi_0(r_p)$, as $x\to x_0$. Thus, Eq. (94) yields

$$\Gamma_1=\nu_0\int\phi_0(r_p)r_p^3K_p^2(r_p)dr_p \tag{95}$$

Similarly,

$$\Gamma_2=\nu_0\int\phi_0(r_p)r_p^3K_p^3(r_p)dr_p \tag{96}$$

and

$$\Gamma_3=\nu_0\theta\int\phi_0(r_p)r_p^3K_p(r_p)L_p(r_p)dr_p \tag{97}$$

Also, it holds true that

$$\frac{\dot{m}_p(r_p)}{\dot{M}_g}=\phi_0(r_p)r_p^3K_p(r_p) \tag{98}$$

Therefore, $\dot{m}_p(r_p)/\dot{M}_g$ appearing in Eqs. (67), (76) etc. may be replaced by Eq. (98). As mentioned previously, in our calculation, the non-equilibrium flow is treated on the assumption that all the particles are in velocity and thermal equilibrium with the gas only near the reservoir. Hence, we note that $K_p(r_p)=1$ and $L_p(r_p)=1$ are adopted for all r_p in the equilibrium region.

4. Numerical experiments

4. 1 Computational conditions

A few numerical experiments will be performed in order to demonstrate the numerical results concerning the flow properties in a nozzle. For the numerical calculation, a gas-particle mixture composed of air and water-particles is treated. The physical constants as well as the reference conditions adopted in this numerical experiment are listed in Table 1. These parameters are fixed throughout the present paper.

Table 1 Physical constants and reference conditions adopted in numerical experiments. These parameters are fixed throughout the present paper.

Physical constants	Reference conditions
$\bar{\rho}_{mp}=1000[kg/m^3]$	$\bar{T}_0=323[K]$
$\bar{c}_{pp}=4187[J/kg \cdot K]$	$\bar{\mu}_0=2.07\times10^{-5}[Pa \cdot s]$ at $\bar{T}_0$
$\bar{c}_{pg}=1004[J/kg \cdot K]$	$\bar{L}_*=1.0\times10^{-3}[m]$
$\gamma=1.4$	
$Pr=0.7$	
$\delta=0.6$	

It is very difficult to specify the distribution function of the radius of the spherical water-particles mixing in the mist. Then, let it be assumed that $\bar{\phi}_0(\bar{r}_p)$ is somewhat arbitrarily given by

$$\bar{\phi}_0(\bar{r}_p)=\bar{J}\bar{r}_p\exp\left(-\frac{\bar{r}_p^2}{250}\right) \tag{99}$$

where $\bar{J}$ is the normalizing factor. If it is assumed that the minimum and the maximum radii of the particles contained in the mixture are specified as

$$\bar{r}_{p,min}=1.0[\mu m] \quad \text{and} \quad \bar{r}_{p,max}=50[\mu m],$$

we have $\bar{J}=1/124.580[\mu m^{-2}]$. Again, the average radius $\bar{l}_{p0}$ has been found to be $17.396[\mu m]$, and the continuous distribution of the particle size from $1[\mu m]$ up to $50[\mu m]$ is represented by eleven discrete sizes so that the size interval may be constant. Each size is made dimensionless according to the definition by $r_p(i)=\bar{r}_p(i)/\bar{l}_{p0}$ $(i=1 \sim 11)$. Table 2 indicates the size number i, $r_p(i)$ and $\phi_0\{r_p(i)\}$.

The two cases are considered in our numerical experiments, one of which corresponds to the case where the gas velocity does not reach the sonic state throughout the whole nozzle length. In this case, the specified area method is applicable to the determination of the gas velocity (see Eq. (76)). The other corresponds to the case where the

Table 2 Size number i, dimensionless particle radius and continuous distribution function.

i	$r_p(i)$	$\phi_0(r_p(i))$
1	0.0575	0.1391
2	0.3392	0.7168
3	0.6208	0.9458
4	0.9025	0.8179
5	1.1842	0.5269
6	1.4658	0.2642
7	1.7475	0.1053
8	2.0292	0.0337
9	2.3108	0.0087
10	2.5925	0.0018
11	2.8742	0.0003

gas velocity is beyond the sonic state, and the specified pressure method is applied for determining the gas velocity (see Eq. (77)). In this case, the pressure profile should be provided over the whole length of the nozzle axis. If so, the nozzle geometry can be designed in accord with the pressure profile.

4. 2 Numerical results of subsonic nozzle flow

First, the nozzle geometry should be given. Here, the sectional area of the nozzle is assumed to consist of the two regions from the reservoir to the nozzle exit as

$$\left.\begin{aligned} &\text{in the region of } x<0; \quad A=\frac{1}{5}x^2+1 \\ &\text{in the region of } 0\leqq x\leqq X_E; \quad A=1 \end{aligned}\right\} \quad (100)$$

in which $X_E=25$ is adopted. Also, we set $\bar{L}_*=1.0[\mathrm{mm}]$ throughout the present paper.

Here, the case is treated where $\bar{p}_0=1.8\times10^5[\mathrm{Pa}]$ at the reservoir. Figure 1 (a), (b) and (c) gives the variation of the pressure, velocity and temperature of the gas-phase along the nozzle axis x with ν as a parameter. It should be kept in mind that $\nu=0$ corresponds to the gas-only flow. It can be seen from these figures that p and T remain almost unvaried from the reservoir up to a certain position, but they rapidly change as x attains zero. Also, V is seen to grow very gradually from the reservoir up to a certain position, and then to increase rapidly as $x\to0$. In the region where the sectional area of the nozzle is constant ($A=1$), (Hereafter, this will be called the parallel region.) the variational behaviours of p, V and T are observed to be relatively smooth. In particular,

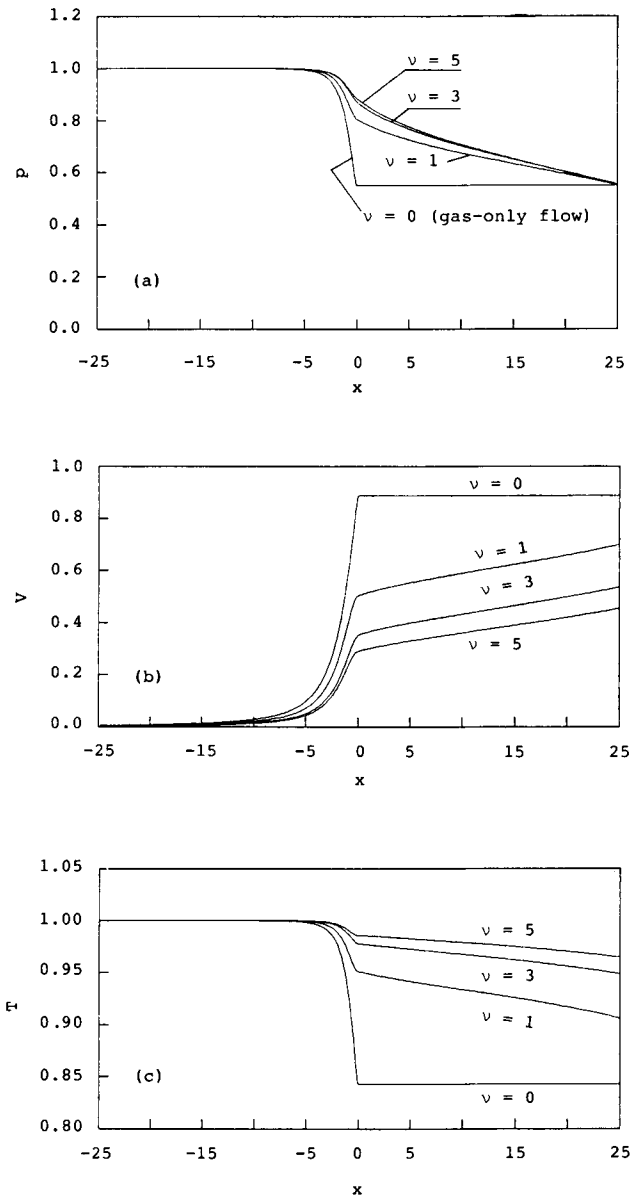

Figure 1 Variation of pressure (a), velocity (b) and temperature (c) of gas-phase along the nozzle axis. Note that $\bar{p}_0=1.8\times10^5$[Pa] and $\bar{p}_e=1.0\times10^5$[Pa], and that the gas-phase pressure in the mixture flow is conditioned to be equal to the ambient gas pressure ($=\bar{p}_e$) at the nozzle exit.

for the case where $\nu=0$, p, V and T remain unvariable in the parallel region. p is at a higher state with ν, while V is at a lower state. One should bear in mind that the gas-phase pressure in the mixture flow is taken to be equal to the ambient gas pressure ($\bar{p}_e=1.0\times10^5$[Pa]) at the nozzle exit (at $x=X_E$), and that $\dot{M}_g$ is determined in such a way as to satisfy the condition.

Figure 2 (a), (b) and (c) gives the variation of the particle velocity $V_p|r_p(i)|$ (i : size number, see Table 2) along the nozzle axis x. It can be observed that $V_p|r_p(i)|$ is increased with x, and the particles of a smaller size tend to travel at a higher velocity. Also, when ν is decreased, $V_p|r_p(i)|$ increases.

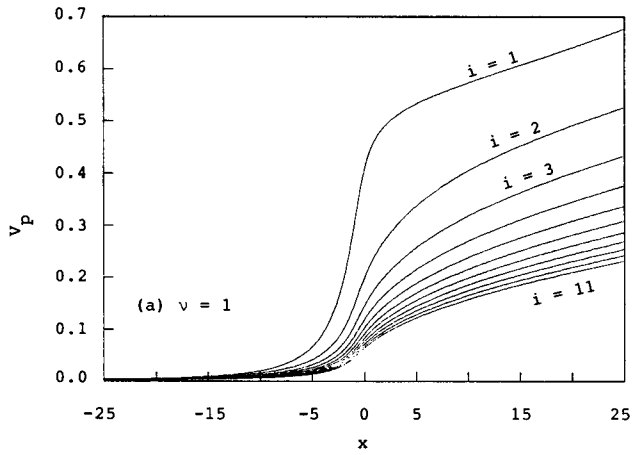

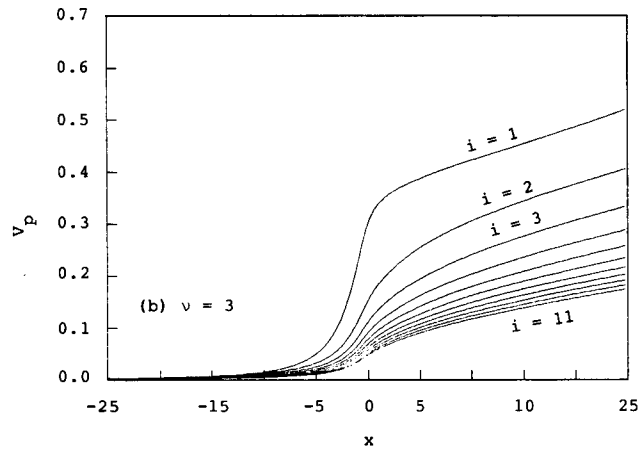

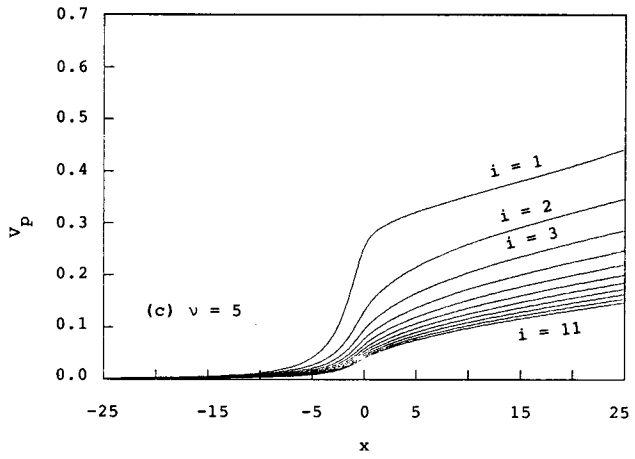

Figure 2 Variation of particle velocities along nozzle axis for $\nu=1.0$ (a), $\nu=3.0$ (b) and $\nu=5.0$ (c). Note that i is the size number to present the particle radius (see Table 2).

Figure 3 (a), (b) and (c) indicates the relation between $K_p\{r_p(i)\}$ (see Eq. (78)) and x. The slip ratio is changeable along x, depending upon the particle size.

Figure 4 (a), (b) and (c) exhibits the variation of $L_p\{r_p(i)\}$ with x. The variational behaviour of $L_p(r_p)$ is observed to be similar to that of $K_p(r_p)$ in the form. $L_p(r_p)$ as well as $K_p(r_p)$ takes the minimum value near $x=0$.

Figure 5 shows the variation of N_p with x. It can be seen that N_p increases in the region of $x<0$, takes the peak value near the entrance of the parallel region (at $x\cong 0$), and then decreases as $x \to X_E$.

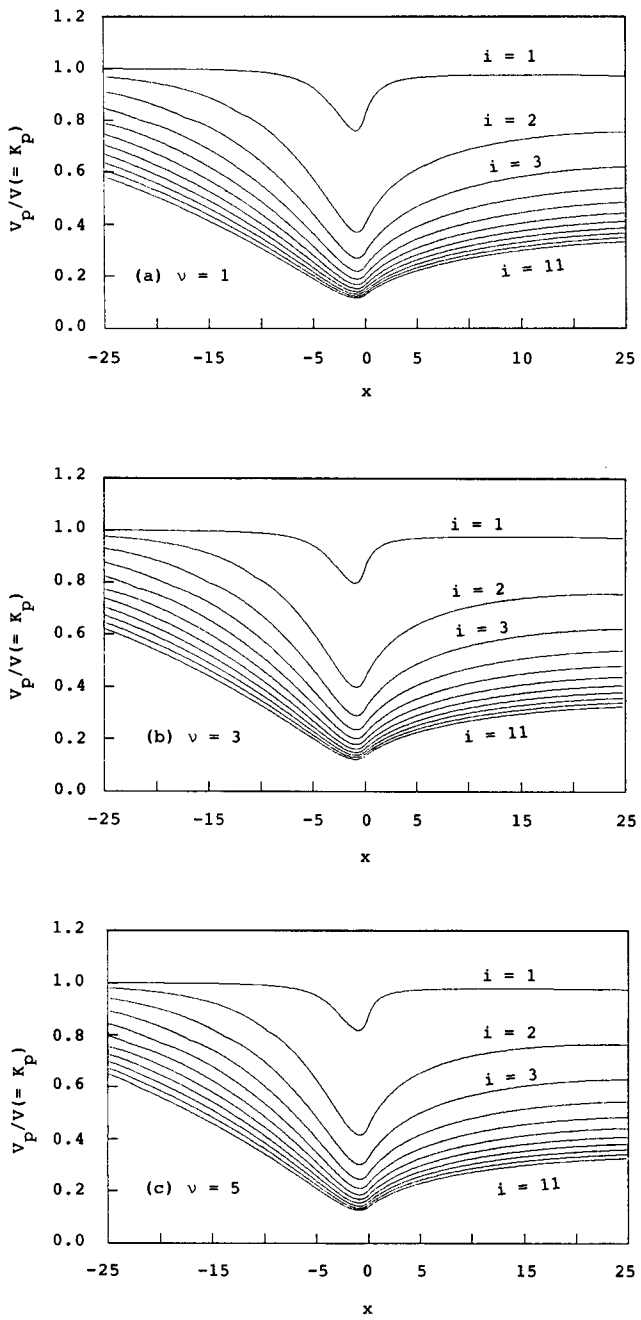

Figure 3 Variation of slip ratio, defined in Eq. (78), with nozzle axis for $\nu=1.0$ (a), $\nu=3.0$ (b) and $\nu=5.0$ (c) (i : size number).

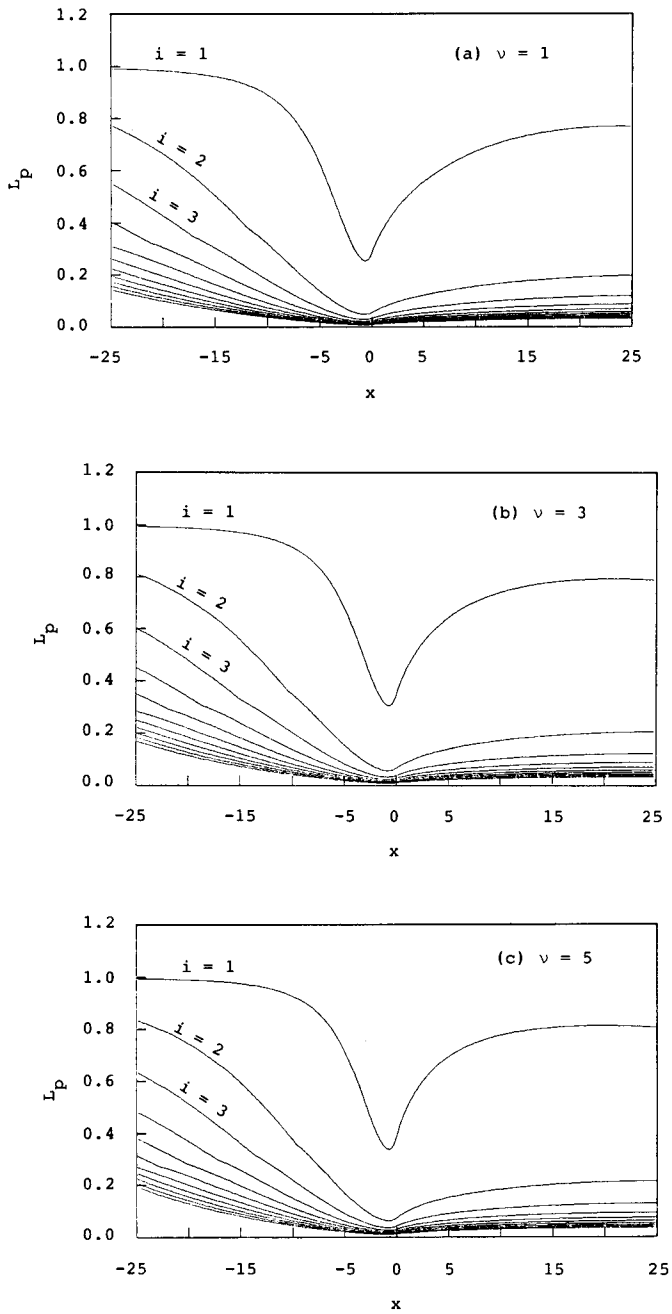

Figure 4 Variation of thermal lag factor L_p, defined in Eq. (79), along nozzle axis for $\nu=1.0$ (a), $\nu=3.0$ (b) and $\nu=5.0$ (c).

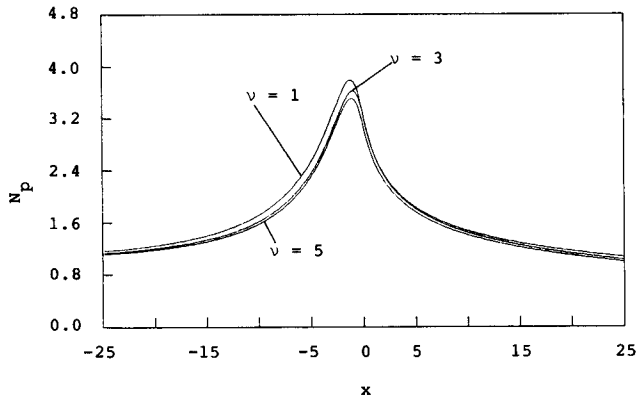

Figure 5 Distribution of total number of particles per unit volume along nozzle axis.

4. 3 Numerical results of supersonic nozzle flow

First, a pressure profile is given, such that p reaches unity as $x \to x_0$ and $p=0.1$ at $X_E=25$. Here, the following pressure profile,

$$p=-k_1\frac{g(x)}{[|g(x)|^2+1]^{1/2}}+(1-k_1)\,;\quad g(x)=k_2x+k_3 \tag{101}$$

is adopted. Here, $k_1=0.451000$, $k_2=0.421457$ and $k_3=0.046614$. We note that $p=0.528$ at $x=0$ and the position of $x=0$ corresponds to that of the throat for the gas-only flow. Figure 6 indicates the variation of p with x.

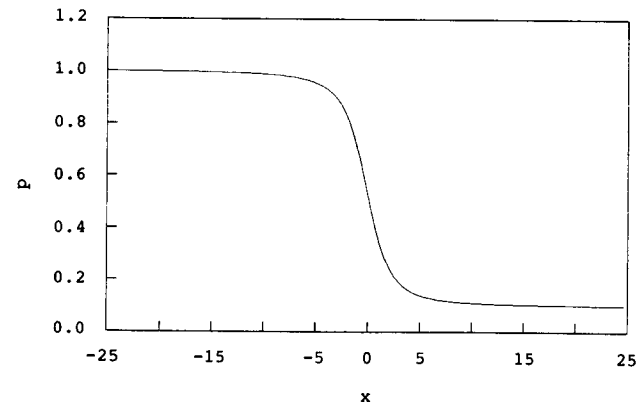

Figure 6 Pressure profile along nozzle axis adopted. Note that this profile was previously given as a function of x, and corresponds to Eq. (101).

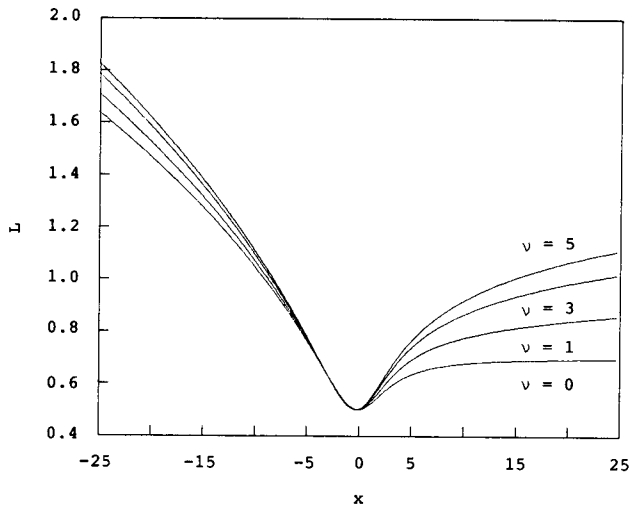

Figure 7 Nozzle geometry calculated according to pressure profile shown in Fig. 6. Note that $\bar{p}_0=10.0\times10^5$[Pa] for the supersonic nozzle flow and $\bar{p}_e=1.0\times10^5$[Pa], and that the gas-phase pressure in the mixture flow is taken to be equal to the ambient gas pressure ($p_e=0.1$).

For the supersonic nozzle flow, the case is considered where $\bar{p}_0=10.0\times10^5$[Pa] at the reservoir. Figure 7 indicates the variation of L with x, that is, the nozzle configuration along the nozzle axis, with ν as a parameter. In this figure, it should be noted that $\nu=0$ corresponds to the gas-only flow, and that the throat is not located at $x=0$, except for the case of $\nu=0$. The throat exhibits the tendency to be located at the slightly negative side of x with the increase in ν (at $x=-0.102$ for $\nu=1$, at $x=-0.185$ for $\nu=3$ and $x=-0.244$ for $\nu=5$). It can be seen from this figure that L is extended in the convergent as well as divergent parts with an increase of the loading ratio.

Figure 8 (a), (b) and (c) gives the variation of V, T and ρ along x, with ν as a parameter. We note that the indication of these flow properties exactly obeys the axis of the nozzle configuration shown in Figure 7, particularly in the case where $\nu=0$, $T_*=0.833$ and $\rho_*=0.634$ at the throat ($A_*=1$). The values coincide with those calculated from $T_*=2/(\gamma+1)$ and $\rho_*=p_*^{1/\gamma}$ ($=T_*^{1/(\gamma-1)}$; $p_*=0.528$). When $\nu=0$, T is seen to decrease rapidly near the throat, and then only gradually decreases as x reaches X_E. This is considered to be due to the isentropic change of gas. Therefore, in this case, V increases also rapidly near the throat, and then very gradually as x attains the nozzle exit (see Fig. 8 (a)), although this is closely related to the pressure profile given in the form of Figure 6. However, it is apparent from these figures that the case where $\nu\neq0$ is different from the case of $\nu=0$. That is, T decreases once rapidly near the throat, and

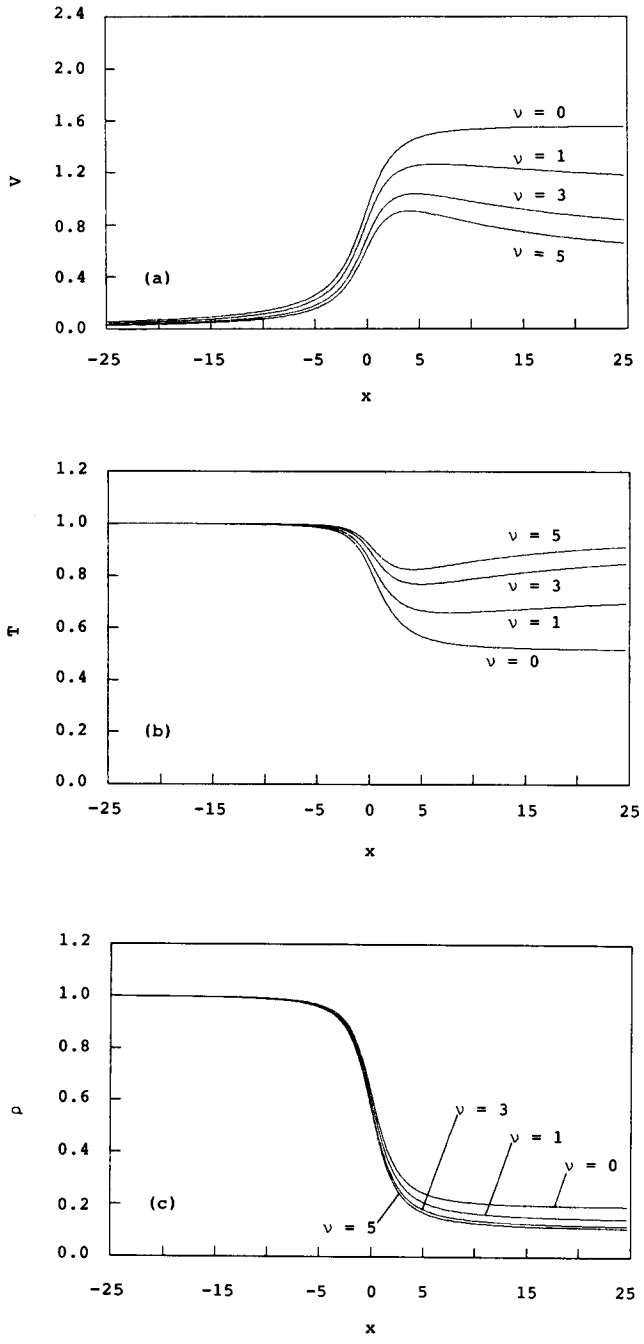

Figure 8 Variation of velocity (a), temperature (b) and density (c) of gas-phase along nozzle axis.

thereafter increases towards the nozzle exit to a considerable degree. Again, T is observed to be higher in the divergent part of the nozzle with the increase in ν. On the other hand, V becomes large sharply near the throat, but somewhat gradually decreases as x reaches X_E. Furthermore, ρ decreases with x in a form similar to the pressure profile. ρ in the case where $\nu \neq 0$ is small in comparison with the case of gas-only flow (see Fig. 8 (c)).

Figure 9 indicates the variation of M ($=V/\sqrt{T}$) against x, with ν as a parameter. For the case where $\nu \neq 0$, the x-axis of $M=1$ is seen to be located downstream from the throat, and such a tendency presents itself in a more conspicuous manner as ν is increased. Also, M increases rapidly near the throat, and then decreases gradually towards

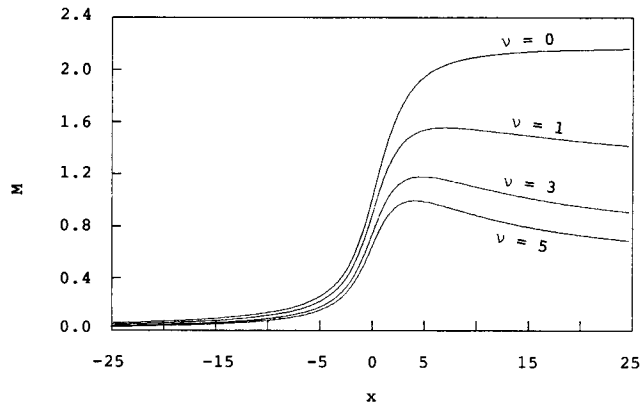

Figure 9 Relation between local gas-phase Mach number and nozzle axis. Note that for $\nu=0$, the x-coordinate of $M=1$ is seen to be located not at the throat, but downstream from the throat.

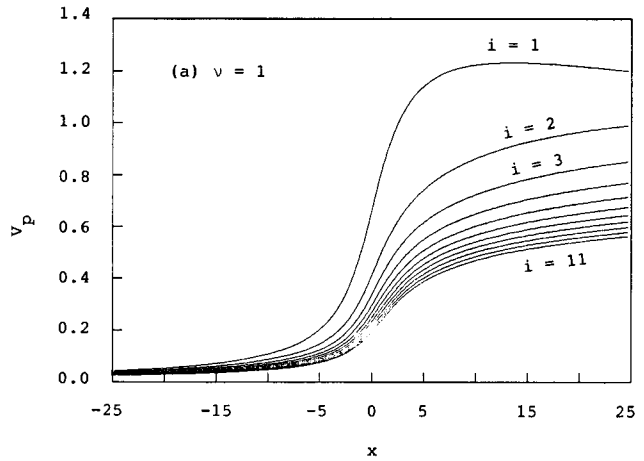

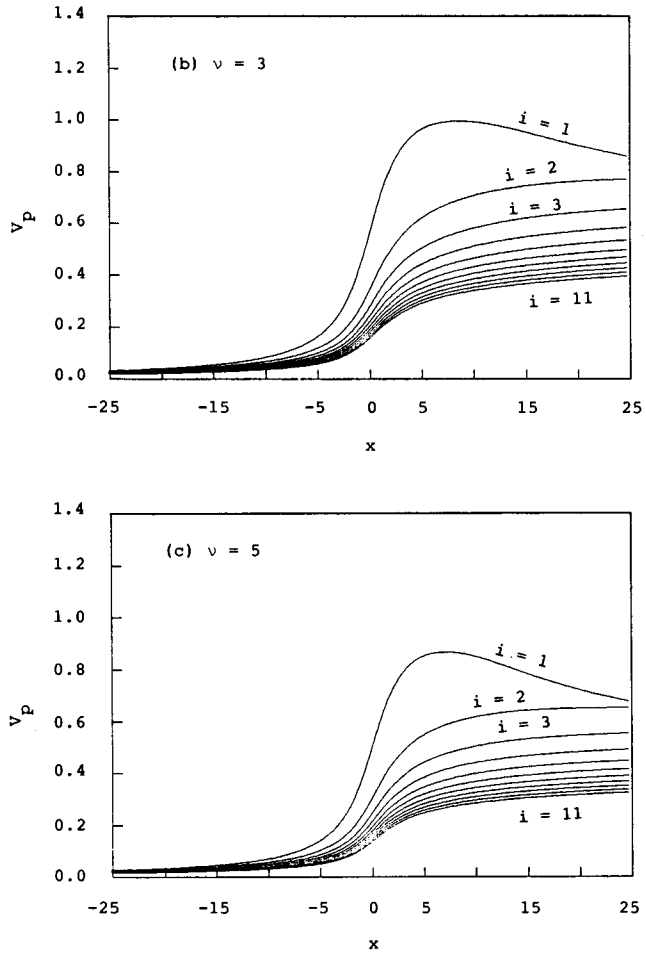

Figure 10 Variation of particle velocities along nozzle axis (i : size number) for $\nu=1.0$ (a), $\nu=3.0$ (b) and $\nu=5.0$ (c).

the nozzle exit for the case where $\nu \neq 0$. The variational behaviour of M against x is similar to that of V in the form.

Figure 10 (a), (b) and (c) gives the variation of $V_p|r_p(i)|$ (i : size number, see Table 2) against x, with i as a parameter. It can be seen from these figures that $V_p|r_p(i)|$ is, as a whole, increased with x, except for the case where $i=1$. Particles wih a smaller radius tend to flow at a higher velocity. Again, the increase in ν brings about the decrease in particle velocities. In addition, it is interesting to note that only the particle velocity profile of $i=1$ is near to the gas velocity profile corresponding to the same loadig ratio.

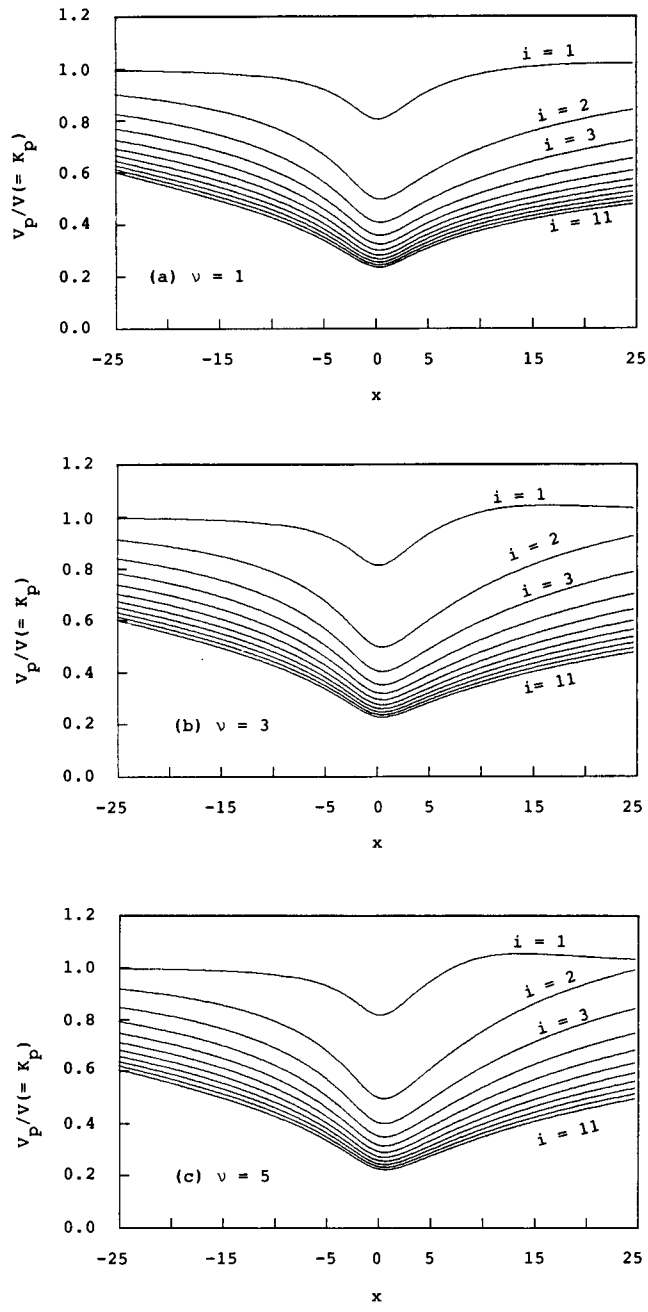

Figure 11 Variation of K_p, defined in Eq. (78), along nozzle axis for $\nu=1.0$ (a), $\nu=3.0$ (b) and $\nu=5.0$ (c) (i : size number).

Figure 11 (a), (b) and (c) shows the variation of $K_p(r_p(i))$ (see Eq. (78)) along x, with i as a parameter. It is clear from these figures that $K_p(r_p)$ becomes higher as r_p becomes smaller. Again, $K_p(r_p)$ decreases in the region from the reservoir to the throat and the inverse occurs downstream from the throat. Furthermore, it should be stressed that the difference in ν does not give a significant change to the slip ratio.

Figure 12 (a), (b) and (c) exhibits the variation of $L_p(r_p)$, defined by Eq. (79), along x, with i as a parameter. This is similar to the case of the slip ratio. $L_p(r_p)$ also decreases upstream from the throat and the opposite occurs downstream from the throat.

Figure 13 shows the relation between N_p and x. It can be seen that N_p increases towards the throat, takes the peak value at the slightly negative side of x, and thereafter decreases towards the nozzle exit.

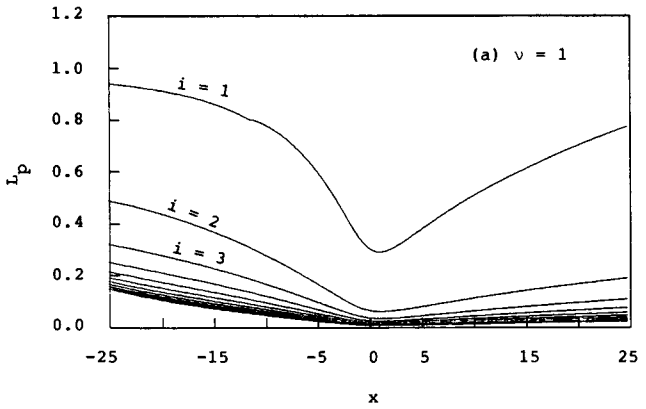

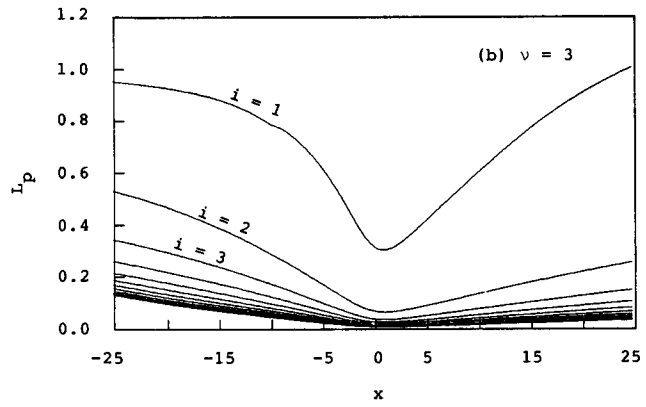

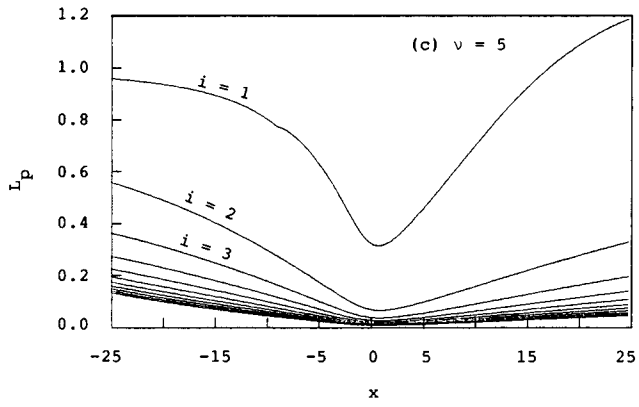

Figure 12 Variation of L_p, defined in Eq. (79), along nozzle axis for $\nu=1.0$ (a), $\nu=3.0$ (b) and $\nu=5.0$ (c) (i : size number).

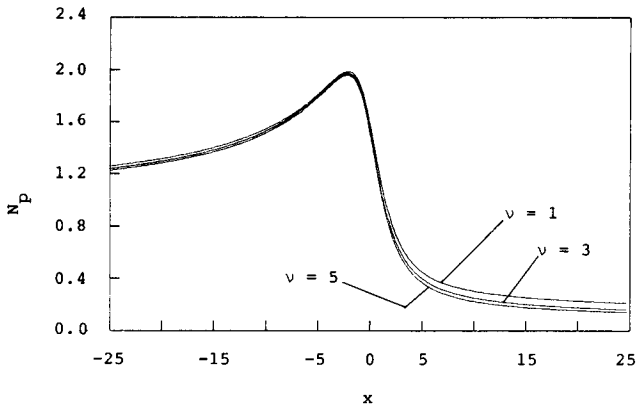

Figure 13 Relation between total number density of particles and nozzle axis.

5. Discussion

According to the theoretical procedure described in the third section, a few calculation examples have been demonstrated.

First, we discuss the numerical results for the subsonic nozzle flow. In this case, all of the flow properties have been calculated on the basis of the nozzle geometry given in Eq. (100). What is remarkable is that the flow properties vary even in the parallel region for the case where $\nu \neq 0$, while for $\nu=0$, p, T and V remain unvaried in the parallel

parallel region.

Now, we wish to discuss the effect of the reservoir pressure $\bar{p}_0$. In order to do so, we treat the case where $\nu=3$. The other computational conditions are the same as the previous case. Figure 14 gives the variation of the local Mach number of the gas-phase

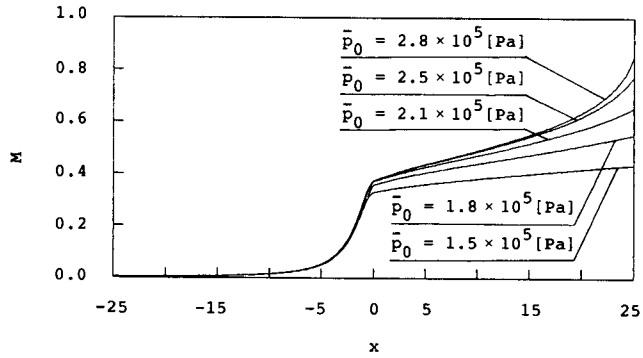

Figure 14 Variation of local gas-phase Mach number along nozzle axis with $\bar{p}_0$ as a parameter ($\bar{p}_e=1.0\times10^5$[Pa] and $\nu=3$). Note that the nozzle geometry given by Eq. (100) is adopted in this calculation.

along the nozzle axis with $\bar{p}_0$ as a parameter. It can be seen from this figure that M reaches unity at $x=X_E$ with the increase in $\bar{p}_0$. As mentioned above, Eq. (76) is singular in the transonic region. Therefore, when the supersonic nozzle flows are treated for a given nozzle geometry, the specified area method should be employed upstream and downstream from that region. The specified pressure method should be employed in the transonic region. That is, first, at a given upstream point, the specified pressure method is adopted as a perturbation from the numerical results obtained by the specified area method. Second, at a certain downstream point, the specified area method is adopted as a perturbation from the numerical results obtained by the specified pressure method. However, if the pressure profile to be predicted in the transonic region is not appropriate for the latter perturbation from the results calculated by the specified pressure method, one should keep in mind that the inconvenient gap occurs between the calculated nozzle sectional area and the previously determined area. This problem will be reported elsewhere.

In the present case, we confine our interest to the subsonic flow regime. Again, the increase in $\bar{p}_0$ leads not only to promoting the gas-phase velocity as well as the particle-phase velocity, but also to increasing the mass flow rates of the two phases regardless of the magnitude of ν[5].

Again, it should be emphasized that the aforementioned system of equations gov-

erning the non-equilibrium flow has been solved as a perturbation from an equilibrium reference flow. The position where V is given by $0.001\,|2/(1+\gamma)|^{1/2}$ is regarded as the end point of the equilibrium region.

Next, we discuss the numerical results for the supersonic nozzle flow. Using the pressure profile given by Eq. (101), it has been shown that the nozzle geometry can be designed in obedience to the desired pressure profile. At the same time, it has been demonstrated that all of the flow properties in the whole region from the subsonic flow to the supersonic flow can be obtained according to the pressure profile given previously along the nozzle axis.

Here, let us prove that $\dot{M}_p=\dot{M}_g$ in the dimensionless space. It holds true from Eqs. (12) and (32) that

$$\bar{\dot{M}}_g=\bar{\rho}\bar{V}\bar{A} \quad \text{and} \quad \bar{\dot{M}}_p=\bar{R}_p\bar{V}\bar{A}$$

on the condition that $V_p(r_p)=V$ in the equilibrium region. Hence,

$$\nu=\frac{\bar{\dot{M}}_p}{\bar{\dot{M}}_g}=\frac{\bar{R}_p}{\bar{\rho}}=\frac{\bar{R}_{p0}}{\bar{\rho}_0}=\nu_0 \tag{102}$$

It is clear, comparing the above relation with Eq. (49), that $\dot{M}_p=\dot{M}_g$. That is, the mass flow rate of the particle-phase is equal to that of the gas-phase in the dimensionless space. It can be said that this is true also for the subsonic nozzle flow. However, it does not hold true that $\bar{\dot{M}}_g=\bar{\dot{M}}_p$ in the dimensional space.

Again, it should be noted that $\dot{M}_p$ decreases with the increase in ν. In the present numerical experiments $\dot{M}_p=0.49908$ at $\nu=1$, $\dot{M}_p=0.40702$ at $\nu=3$ and $\dot{M}_p=0.35271$ at $\nu=5$ for the supersonic nozzle flow. From Eq. (46),we have.

$$\bar{\dot{M}}_g=\dot{M}_g\bar{p}_0\bar{A}_*(\gamma/\bar{R}\bar{T}_0)^{1/2} \quad \text{and} \quad \bar{\dot{M}}_p=\nu\bar{\dot{M}}_g \tag{103}$$

Thus, $\bar{\dot{M}}_p=6.09\times10^{-3}$ [kg/s] at $\nu=1$, $\bar{\dot{M}}_p=0.0149$ [kg/s] at $\nu=3$ and $\bar{\dot{M}}_p=0.0215$ [kg/s] at $\nu=5$. In passing, for the above subsonic nozzle flow, $\dot{M}_p=0.42593$ at $\nu=1$, $\dot{M}_p=0.31366$ at $\nu=3$ and $\dot{M}_p=0.25894$ at $\nu=5$. Again, $\bar{\dot{M}}_p=9.36\times10^{-4}$ [kg/s] at $\nu=1$, $\bar{\dot{M}}_p=2.06\times10^{-3}$ [kg/s] at $\nu=3$ and $\bar{\dot{M}}_p=2.86\times10^{-3}$ [kg/s] at $\nu=5$.

Finally, the position where $p=0.994$ has been regarded as the end point of the equilibrium region. Therefore, we should like to emphasize that the perturbation between the equilibrium and the non-equilibrium flows has been made at the above position for the supersonic nozzle flow.

6. Conclusion

We have constructed a system of equations governing the nozzle flow of gas-

particle mixture to evaluate all of the flow properties in the flow field. It has been stressed that the equation to determine the gas-phase velocity plays an important role from the point of view of the numerical treatment. Eq. (76) is clearly singular in the transonic region. Therefore, for the subsonic nozzle flow, all of the flow properties have been calculated on the basis of the nozzle geometry with the parallel region by the specified area method. What is remarkable is that the flow properties vary even in the parallel region for the case $\nu \neq 0$, while for $\nu = 0$, the pressure, temperature and velocity of the gas-phase remain unvaried in the parallel region.

Next, for the supersonic nozzle flow, the specified pressure method has been employed by a pressure profile given along the nozzle axis. All of the flow properties in the whole region from the subsonic flow to the supersonic flow have been obtained in accord with the given pressure profile. Again, it has been demonstrated that the nozzle configuration can be designed according to the desired pressure profile.

In conclusion, we note that the theoretical procedure mentioned here has the attractive aspect whereby the nozzle flow of the gas-particle mixture can be exactly understood from a numerical point of view.

Acknowledgement

The authors would like to note that this study has been supported through the Grant in Aid for Scientific Research (01550532) of the Ministry of Education, Science and Culture in Japan.

References

1) J. R. Kliegel : "Gas Particle Nozzle Flows" 9th Int. Symp. on Combustion, Academic Press, New York, (1963), 811.
2) I. Shin Chang : AIAA Journal, 18 (1980), 1455.
3) R. Ishii and Y. Umeda : Phys. Fluids, 30 (1987), 752.
4) M. J. Zucrow and J. D. Hoffman : "Gas Dynamics (Vol. 2)", John Wiley and Sons, (1977), 53.
5) N. Hatta, R. Ishii, H. Takuda, K. Ueda and J. Kokado : Trans. ISIJ., 28 (1988), 930.
6) N. Hatta, H. Takuda, R. Ishii and H. Fujimoto : ISIJ Int., 29 (1989), 605.
7) C. B. Henderson : AIAA Journal, 14 (1976), 707.
8) D. J. Carlson and R. F. Hoglund : AIAA Journal, 2(1964), 1980.